ACS OMEGA

http://pubs.acs.org/journal/acsodf

Article

Choline [Amino Acid] Ionic Liquid/Water Mixtures: A Triple Effect for the Degradation of an Organophosphorus Pesticide

Paulina Pavez,* Roberto Figueroa, Mayte Medina, Daniela Millán, R. Darío Falcone, and Ricardo A. Tapia

Cite This: *ACS Omega* 2020, 5, 26562−26572

Read Online

ACCESS | Metrics & More | Article Recommendations | Supporting Information

ABSTRACT: A series of ionic liquids (ILs) composed by choline (Ch) as a cation and different amino acids (AA) as anions and their respective aqueous mixtures were prepared using different [Ch][AA] contents in a range of 0.4−46 mol % IL. These solvents were used for the first time to achieve an eco-friendlier Paraoxon degradation. The results show that [Ch][AA]/water mixtures are an effective reaction medium to degrade Paraoxon, even when the IL content in the mixture is low (0.4 mol % IL) and without the need of an extra nucleophile. Both the kinetics and the degradation pathways of pesticides depend on the nature of the AA on [Ch][AA] and the amount of an IL present in the mixture. We have demonstrated that in those mixtures with a low amount of [Ch][AA], the hydrolysis reaction is the main pathway for Paraoxon degradation, showing a catalytic effect of the IL. However, as the percentage of [Ch][AA] increases in the mixture, the nucleophilic attack of [Ch][AA] is evident. Finally, the aim of this study was to provide evidence of a promising and biocompatible methodology to degrade a toxic compound (Paraoxon) using a minimal quantity of an IL designed totally from natural resources.

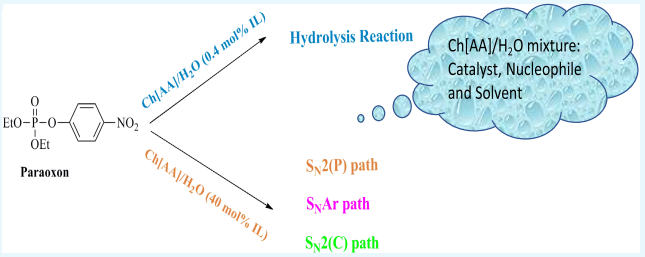

INTRODUCTION

Nowadays, the benefits obtained when ionic liquids (ILs) are used as a reaction medium are undeniable.[1] Due to their main features, they became the best alternative to replace volatile organic solvents in several areas of chemistry.[2] The ILs derived from petroleum, composed of organic cations such as dialkylimidazolium and alkylpyridinium and inorganic anions as hexafluorophosphate [PF_6^-], tetrafluoroborate [BF_4^-], and dicyanamide [DCA^-], have been the most used.[3,4] Nevertheless, two problems arose with the use of ILs mentioned above: the high cost involved in the synthesis and the inherent toxicity of their components (cations and anions, commonly used). These two points have been the major constraints to widespread use of ILs in industry. There are many reports indicating that these ILs are neither sustainable nor biodegradable, and in many cases, they exhibit relatively high toxicity.[5] Some studies indicate that the toxicity can be attributed to both the anion and cation present in the IL.[6,7]

A good strategy to reduce the amount of an IL required to carry out a process or a reaction is to mix ILs with other solvents, such as an organic solvent or even water.[8,9] For example, Harper et al. studied the effect of the variation of the mole fraction of an IL (χIL) in a molecular solvent on the outcome of organic reactions.[10−14] They concluded that the increase in rate constants varying χIL is mainly due to changes in the solvent-solute structures that are occurring between $0 < \chi IL < 0.3$. Besides, considering solvent parameters of ILs, such as Kamlet and Taft, they demonstrated the importance of solvent effects on both the rate- and product-determining steps of the reaction studied.[13,14]

On the other hand, Gholami et al. studied kinetically Diels−Alder reactions of IL/methanol mixtures, and they found that second-order rate constants were enhanced in these mixtures in comparison to neat ILs.[15] However, not only better kinetics results have been observed when adding water or a molecular solvent to ILs; the diffusion coefficient, viscosity, and surface tension of ILs varied considerably upon adding water.[8]

Nevertheless, although the amount of an IL is reduced using IL/solvent mixtures, the toxic components of them still remain being released to the environment. Thus, the preparation of ILs derived from renewable resources can be used as a better strategy in order to obtain a reaction medium with a greener environmental profile. Accordingly, bio-based ILs have appeared as new green solvents.[16−20] For this propose and considering that amino acids (AA) are one of the most abundant resources in nature, they are considered as excellent feedstocks for the synthesis of bio-based ILs. The first amino

Received: July 9, 2020
Accepted: September 23, 2020
Published: October 5, 2020

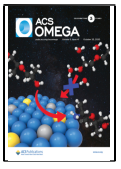

acid-derived ionic liquids (AAILs) were described by Ohno et al., where 1-ethyl-3-methylimidazolium (Emim) was the cation and 20 essential AA were used as anions, ([Emim][AA]).[17] All of them were clear liquids, cheaper, and more biodegradable.[16] Considering the latter, recently, we synthesized a series of ILs using 1-butyl-3-methylimidazolium (Bmim) as a cation and different AA as anions, ([Bmim][AA]).[21] These ILs were used as reaction media on the degradation of an organophosphorus pesticide, Paraoxon. The results show that all neat [Bmim]-[AA] used have a dual role in the outcome of this degradation reaction, as a nucleophile and a solvent to carry out degradation of the organophosphorus pesticide. Therefore, the degradation of Paraoxon is accomplished with great efficiency and without an extra nucleophilic agent.[21]

Nevertheless, to improve more the environmental profile of ILs, it is mandatory that both anion and cation are obtained from natural resources. Keeping this in mind, choline-amino acid ILs ([Ch][AA]) were introduced in 2012 by Liu et al.[22,23] They have enormous potential to improve the green credentials of ILs because they are biodegradable and could be less toxic.[24] The interest in these systems obtained totally from natural and renewable feedstocks has increased significantly, and a large number of papers appeared in the last few years.[22,25] Nevertheless, to date, the use of [Ch][AA] ILs as a reaction media has been less explored, and there is no report about the use of them for degradation of organophosphate pesticides.

Considering the above, we proposed to use [Ch][AA]/water mixtures (approx. 0.4−46 mol % IL) as reaction media for degradation of the organophosphate pesticide Paraoxon. The high viscosity values that present the [Ch][AA] ILs prevent the use of mixtures with higher IL content. The different [Ch][AA] ILs used in this study and schematic degradation of Paraoxon are shown in Scheme 1. The aim of this study was to generate a promising and biocompatible methodology to degrade a toxic compound (Paraoxon) using a minimal quantity of an IL formed totally from natural sources. The proposal involves the application of non-toxic [Ch][AA] ILs and to reduce the amount of an IL by using [Ch][AA]/water mixtures. The results show that both the kinetics and pathways of Paraoxon degradation depend on the nature of the AA present on [Ch][AA] and the amount of an IL used in the mixture.

Scheme 1. Chemical Structure of Synthesized [Ch][AA] and Schematic Degradation of Paraoxon in the Presence of [Ch][AA]/Water Mixtures

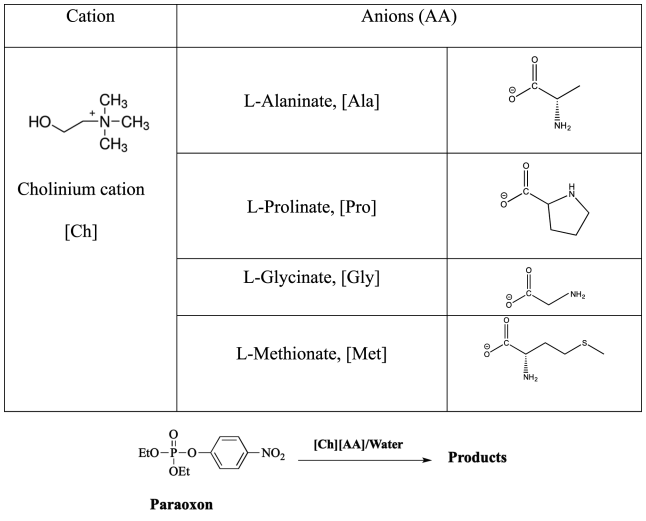

RESULTS AND DISCUSSION

^{31}P Nuclear Magnetic Resonance Study. The study of Paraoxon degradation was performed in [Ch][AA]/water mixtures containing different concentrations of [Ch][AA] from approx. 0.4 to 46 mol % IL, where AA are [Ala], [Gly], [Met], and [Pro]. The effect of each [Ch][AA]/water mixture on the stability of the pesticide Paraoxon was studied using the ^{31}P NMR technique, as it can be observed in Figures S1−S12 in the Supporting Information. The results showed that when Paraoxon was left in [Ch][AA]/water mixtures at room temperature for a few minutes, the pesticide was completely degraded without the need of an extra nucleophile. We previously observed a similar behavior when different neat [Bmim][AA] ILs were used as reaction media for Paraoxon degradation, and it was demonstrated that the AA components of the structure of ILs were responsible for the nucleophilic attack to Paraoxon.[21] Interestingly, in this study, the same nucleophilic effect of the anion present in [Ch][AA] ILs is observed in those mixtures with a percentage of [Ch][AA] in the range of 7−46 mol % IL. However, when the amount of the IL is lower, the mechanism of Paraoxon degradation seems to be different as will be shown later. In this range, the results show that the kinetics and products formed in the Paraoxon degradation depend on the nature of the AA anion and the amount of [Ch][AA] present in the IL/water mixture.

Figure 1 shows the ^{31}P NMR spectra of the Paraoxon degradation in the presence of [Ch][Ala]/water mixtures (35 mol % IL) at different times.

As can be observed, the decrease in the Paraoxon signal (−7.2 ppm) is simultaneous with the increase in four other signals at 8.9, −0.64, −6.3, and −1.8 ppm, which represent the formation of the four new phosphorylated species proposed in Scheme 2. The signal at 8.9 ppm is attributed to phosphorylated species **1a** formed by the nucleophilic attack of the [Ch][Ala] to the phosphorus atom of Paraoxon, and anion 4-nitrophenoxide (**5**) (leaving group) is also formed, see Scheme 2. The presence of **1a** was assigned by comparison with the ^{31}P NMR spectra of the product obtained in the reaction of *O*,*O*-diethyl chlorophosphate with [Ch][Ala] under the same experimental conditions (Figure S13 in the Supporting Information). Besides, the signals at −0.64 and −6.3 ppm were attributed to phosphoryl species **2** and **3** in Scheme 2. These products were identified by ^{31}P NMR comparison with authentic samples; see Figures S14−17 in the Supporting Information; synthesis details of **3** are reported by us in a reference.[26] The presence of **6a** was confirmed from the increase in a band at ∼425 nm in the UV−vis spectra (not shown).

The reactions mentioned above involve nucleophilic attack of [Ch][Ala] at the following electrophilic center of Paraoxon: (i) the phosphoryl center (S_N2(P) path), (ii) the C-1 aromatic carbon (S_NAr path), and (iii) the aliphatic carbon (S_N2(C) path), where the amine group of the alanine anion present in the IL acts as a nucleophile, as shown in Scheme 2.

Besides, as can be observed in Figure 1, a fourth phosphoryl signal at −1.8 ppm is found in [Ch][Ala]/water mixtures (35 mol % IL), which disappears simultaneously with the increase in another new phosphoryl signal at −1.2 ppm. In order to achieve a better understanding, we followed the Paraoxon

https://dx.doi.org/10.1021/acsomega.0c03305
ACS Omega 2020, 5, 26562−26572

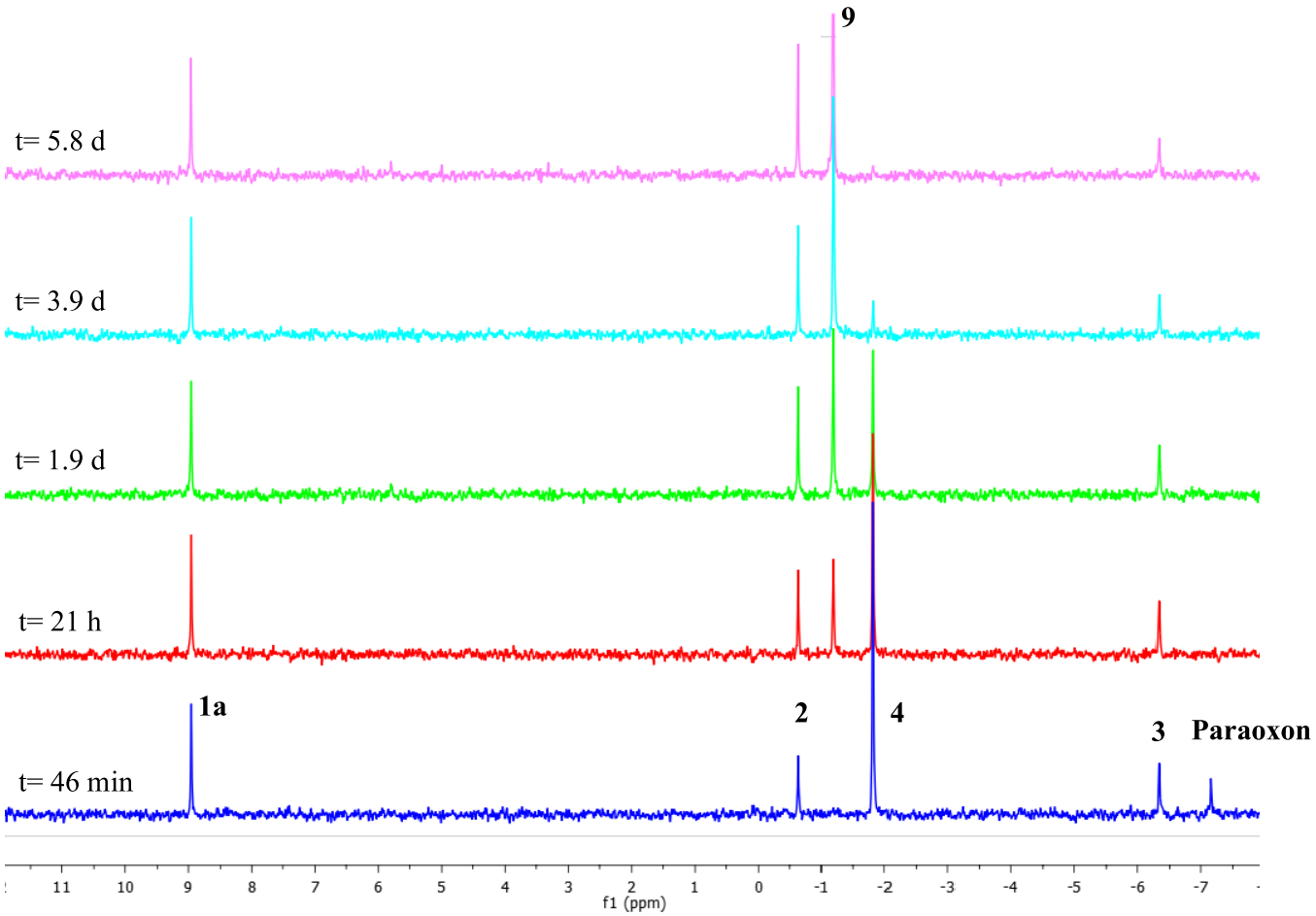

Figure 1. Stacked ^{31}P NMR plots for the reaction of Paraoxon (0.10 M) in [Ch][Ala]/water mixtures (35 mol % IL) at 25 °C.

degradation in the presence of low content of the [Ch][Ala] in the water mixture (1 mol % IL), see Figure 2.

As can be observed in Figure 2, the increase in water concentration in the mixture leads to a downfield shift of ^{31}P NMR signals. The decrease in the Paraoxon signal (−6.6 ppm) is simultaneous with the increase in two new signals at 0.62 and approx. −1.6 ppm. Besides, when the same reaction is followed by UV−vis spectroscopy, a band at 400 nm is evidenced.

In order to understand the full mechanism of Paraoxon degradation in [Ch][Ala]/water mixtures at 1 mol % IL, a product analysis by ESI-MS in the negative mode was performed. Figure 3 shows ESI-MS(−) spectra obtained for Paraoxon degradation in the presence of [Ch][Ala]/water mixtures (1 mol % IL) at an infinite time. The results showed two reaction products. One of them corresponds to compound **2** (Scheme 2) with *m*/*z* of 153.0311 (*m*/*z* calc., 153.0322), and the other corresponds to compound **5** (4-nitrofenolate) with *m*/*z* of 138.0184 (*m*/*z* calc., 138.0187). The $S_N2(P)$ pathway is not observed (no signal at 89.9 ppm), but the presence of compound **5**, in the [Ch][Ala]/water mixture (1 mol % IL), could be explained by two parallel hydrolysis reactions in the Paraoxon degradation: (i) nucleophilic attack of water at the C-1 aromatic carbon forming compounds **2** and **5** and (ii) by the nucleophilic attack of water at the phosphoryl center of Paraoxon, forming compounds **4** and **5** (in Scheme 2), evidenced as reaction products according to ^{31}P NMR and ESI-MS experiments.

It has been described that in aqueous solution, the solvation decreases the nucleophilicity of aliphatic amines.[27] Therefore, it is possible to conclude that in the [Ch][Ala]/water mixtures at 1 mol % IL, probably, the nucleophilicity of alanine anions decreases, and the nucleophilic attacks by water (hydrolysis reactions) are predominant.[28,29]

On the other hand, it is important to remark that when the Paraoxon degradation is performed in [Ch][Ala]/water mixtures at 35 mol % IL, the signal at −1.8 ppm disappears simultaneously with the increase in a new phosphoryl signal at −1.2 ppm, see Figure 1. The latter could be explained by a fast step of deprotonation of **4** giving rise to the new phosphorus signal (−1.2 ppm), attributed to compound **9** in Scheme 2. This fast step of deprotonation was reported previously in the hydrolysis of triethyl phosphate and ethyl acetate.[30]

The Paraoxon degradation showed a similar behavior when [Ch][Met]/water and [Ch][Gly]/water mixtures (with approx. 0.4−46 mol % IL) and [Ch][Pro]/water mixtures (with approx. 1 mol % IL) were used as reaction media; see Figures S1−S10 in the Supporting Information. Nevertheless, when [Ch][Pro]/water mixtures in the range of 7−46 mol % IL (Figures S11and S12 in the Supporting Information) were used as reaction media, a new signal approx. at 6.0 ppm appears slowly in the ^{31}P NMR spectra, as it is shown in Figure 4. The intensity of this signal increases at the expense of compound **3**, forming new phosphoryl compound **8d** (see Scheme 2). This new compound **8d** was confirmed on the basis of the increase in the same signal (approx. at 6.0 ppm) in

https://dx.doi.org/10.1021/acsomega.0c03305
ACS Omega 2020, 5, 26562−26572

Scheme 2. Nucleophilic Attack by [Ch][AA] on Paraoxon via Four Reaction Paths: At the Phosphorylic Center ($S_N2(P)$), at the C-1 Aromatic Carbon (S_NAr), at the Aliphatic Carbon of Paraoxon ($S_N2(P)$), and a New Nucleophilic Attack of Water Present in the [Ch][AA]/Water Mixture (Hydrolysis Reaction)

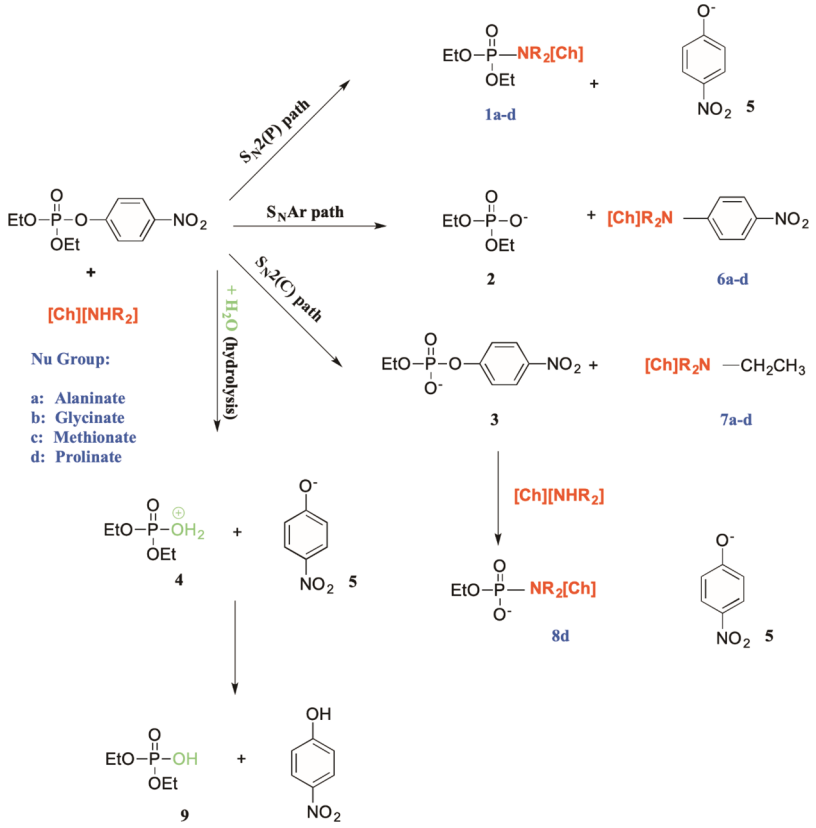

the reaction of *O*-ethyl 4-nitrophenyl phosphate monoester (**3**) with [Ch][Pro] under the same experimental conditions (not shown). Therefore, the formation of compound **8d** is attributed to a second nucleophilic attack of [Ch][Pro] to the phosphorous atom of compound **3**, see Scheme 2. The formation of a phosphate diester derivative (compound **8d**) under these experimental conditions generates a less lipophilic product than Paraoxon and therefore less toxic.

From integration of the ^{31}P NMR signals of the products formed in the Paraoxon degradation in the presence of each [Ch][AA]/water mixture used in this study (Figures S1−S12 in the Supporting Information), the relative product distribution was calculated in the different [Ch][AA]/water mixtures, as shown in Table S1 in the Supporting Information. Figure 5 shows this behavior schematically.

As can be observed in Figure 5, two effects on the product distribution obtained in Paraoxon degradation are evidenced, (a) the effect of the amount of an IL in the mixture and (b) the effect of the nature of AA present as anions in each IL.

In the mixtures [Ch][Ala]/water, [Ch][Gly]/water, and [Ch][Met]/water with low content of ILs (0.4−1 mol % IL), the Paraoxon degradation occurs only by hydrolysis reactions, where the solvation of water decreases the nucleophilicity of the AA present in the each [Ch][AA]. Interestingly, as the percentage of [Ch][AA] increases in the mixture, the nucleophilic attack of [Ch][AA] is evidenced, and the Paraoxon degradation occurs by three parallel pathways, nucleophilic attack of [Ch][AA] by $S_N2(C)$ and S_NAr pathways and hydrolysis reaction (see Figure 5). Finally, in those [Ch][AA]/water mixtures with a higher amount of ILs (30−46 mol % IL), the Paraoxon degradation occurs by all pathways shown in Scheme 2 ($S_N2(P)$, $S_N2(C)$, S_NAr pathway, and hydrolysis pathway). These results suggest a catalytic effect of [Ch][AA] in the hydrolysis reaction of Paraoxon in those mixtures with low content of ILs, as we will explain below.

On the other hand, in all [Ch][Pro]/water mixtures, the Paraoxon degradation occurs by four reaction pathways even in those mixtures with a low percentage of [Ch][AA] (1 mol % IL). Besides, as the amount of ILs increases in the [Ch][Pro]/water mixtures, the $S_N2(P)$ pathway is favored, while the Paraoxon hydrolysis pathway decreased.

These results are highly interesting because it is possible to completely degrade Paraoxon in an aqueous medium and additionally to handle the degradation products by choosing the different [Ch][AA]/water mixtures used in this study.

Kinetics Study. The kinetics study of Paraoxon degradation was performed in mixtures containing a range of different [Ch][AA] contents from approx. 0.4 to 20 mol % IL. It is important to note that a kinetics study at higher concentrations of [Ch][AA] was not possible due to the high viscosity value that presents the [Ch][AA] ILs.[31]

The kinetics study was followed spectrophotometrically by measuring the absorbance increase at 400−420 nm. Pseudo-first-order rate constants (k_{obsd}) were obtained considering the excess of the nucleophile ([Ch][AA]). These rate constants and the experimental conditions are shown in Tables S2−S5 in the Supporting Information.

The kinetics law obtained in the present reactions is given by eq 1, where k_{obsd} is the pseudo-first-order rate coefficient and k_1 is strictly k'_2 [water]. k'_2 and k_2 are the rate coefficients for

https://dx.doi.org/10.1021/acsomega.0c03305
ACS Omega 2020, 5, 26562−26572

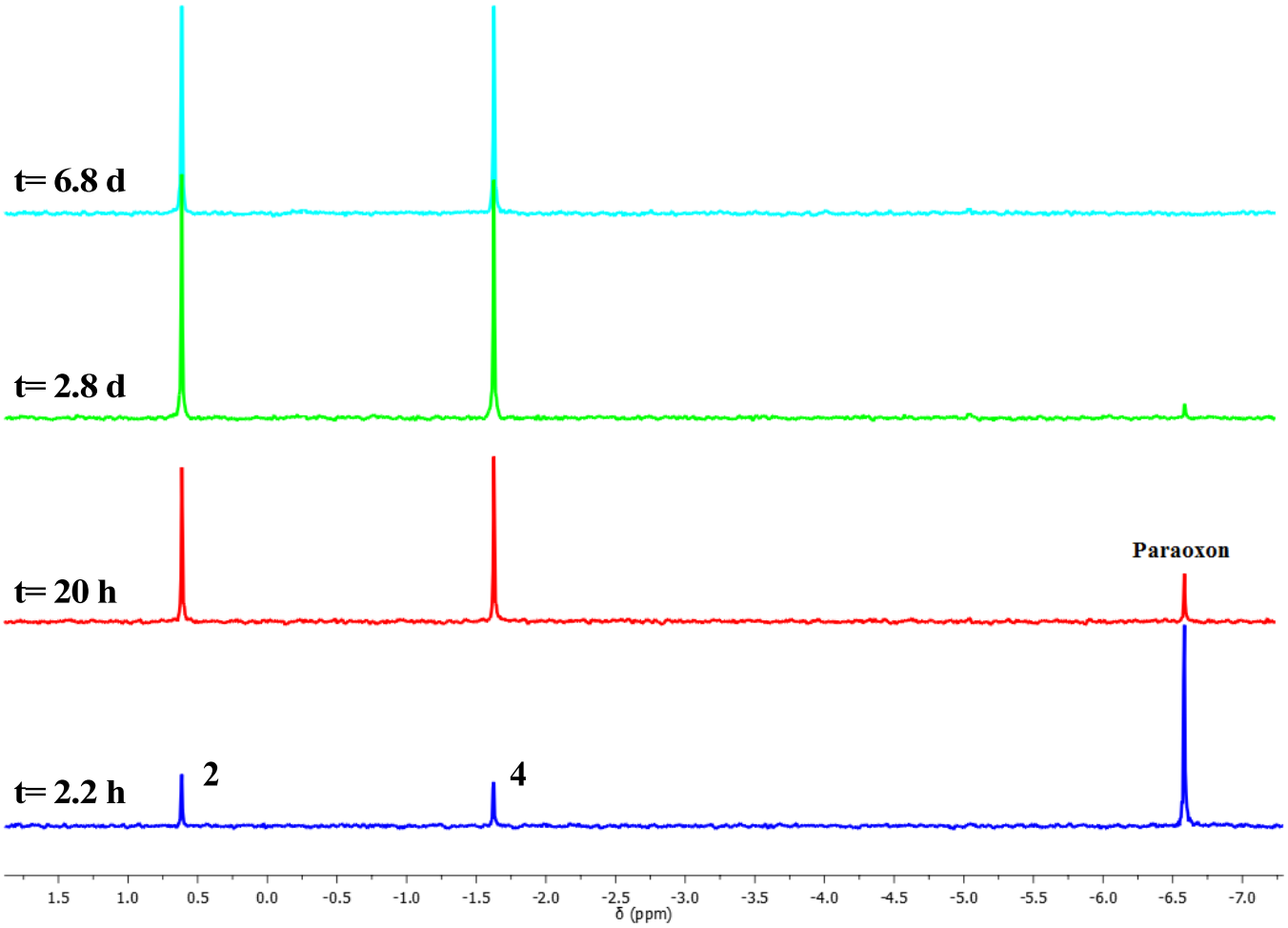

Figure 2. Stacked ^{31}P NMR plots for the reaction of Paraoxon (0.10 M) in [Ch][Ala]/water mixtures (1 mol % IL) at 25 °C.

hydrolysis and for the nucleophilic attack by the [Ch][AA], respectively.

$$k_{obsd} = k_1 + k_2[[Ch][AA]] \quad (1)$$

Considering a water concentration of 55 M, the values k'_2 were calculated as the intercept, and k_2 values were obtained as the slope of linear plots of k_{obsd} vs. [Ch][Ala] mol % present in each mixture. Then, with the rate constant values (k'_2 and k_2), the $t_{1/2}$ values for both processes were calculated ($t_{1/2}$ = ln 2/k'_2 or k_2) and are shown in Table S6 in the Supporting Information. The results show that the $t_{1/2}$ values for the hydrolysis of Paraoxon in the absence of ILs vary from 7 to 15 days in accordance with that reported in the literature.[32]

As an example, Figure 6a shows plots of k_{obsd} against [Ch][Ala] mol % present in the mixture. An increase in k_{obsd} values of at least one magnitude as the [Ch][Ala] content in the mixture increases from 0.4 to 20 mol % can be observed. Similar results are found in [Ch][Gly]/water, [Ch][Met]/water, and [Ch][Pro]/water mixtures and are shown in Figures S18−S21 in the Supporting Information.

Considering the linear correlation between k_{obsd} values and [Ch][AA] mol % present in the mixtures, shown in Figure 6a and Figures S18−S21 in the Supporting Information, we have extrapolated the k_{obsd} values for Paraoxon degradation at 1, 20, and 100 mol % IL for each [Ch][AA]. From these k_{obsd} values, the half-life values ($t_{1/2}$, min) are calculated ($t_{1/2}$ = ln 2/k_{obsd}) and shown in Table 1. Besides, in order to compare these results, we have included in Table 1 the $t_{1/2}$ values reported in neat [Bmim][AA].[21]

As can be observed in Table 1, the kinetics results found in [Ch][AA]/water mixtures at 1 mol % IL showed that the Paraoxon degradation is obtained efficiently with $t_{1/2}$ values between 2 and 3 h. It is important to note that the $t_{1/2}$ values reported for the hydrolysis reactions of several organophosphorus pesticides in aqueous solution varies from 4 to 192 days, depending on experimental conditions, such as pH and temperature.[32] Therefore, in this study, we have demonstrated a notable decrease in $t_{1/2}$ values for Paraoxon hydrolysis up to three orders of magnitude less in comparison with those $t_{1/2}$ values reported in aqueous solution.[32]

Besides, the results showed that the $t_{1/2}$ values found for hydrolysis of Paraoxon in the presence of (1 mol % IL) are lower than those found for the hydrolysis process in the absence of ILs (see $t_{1/2}$ values calculated by using k'_2 values in Table S6 in the Supporting Information).

The results obtained in this study could suggest a catalytic effect of [Ch][AA] in those mixtures with a low amount of ILs (0.4−1 mol % IL), through hydrogen bonding interaction that stabilizes a transition state (TS) for the nucleophilic attack of water to the phosphoryl center of Paraoxon, as shown in Figure 7. Whereas the hydroxyl group of the cholinium cation establishes one hydrogen bond with the oxygen of the phosphoryl group of Paraoxon, the nucleophilic attack of water at the phosphoryl center is favored. Besides, the amino

https://dx.doi.org/10.1021/acsomega.0c03305
ACS Omega 2020, 5, 26562−26572

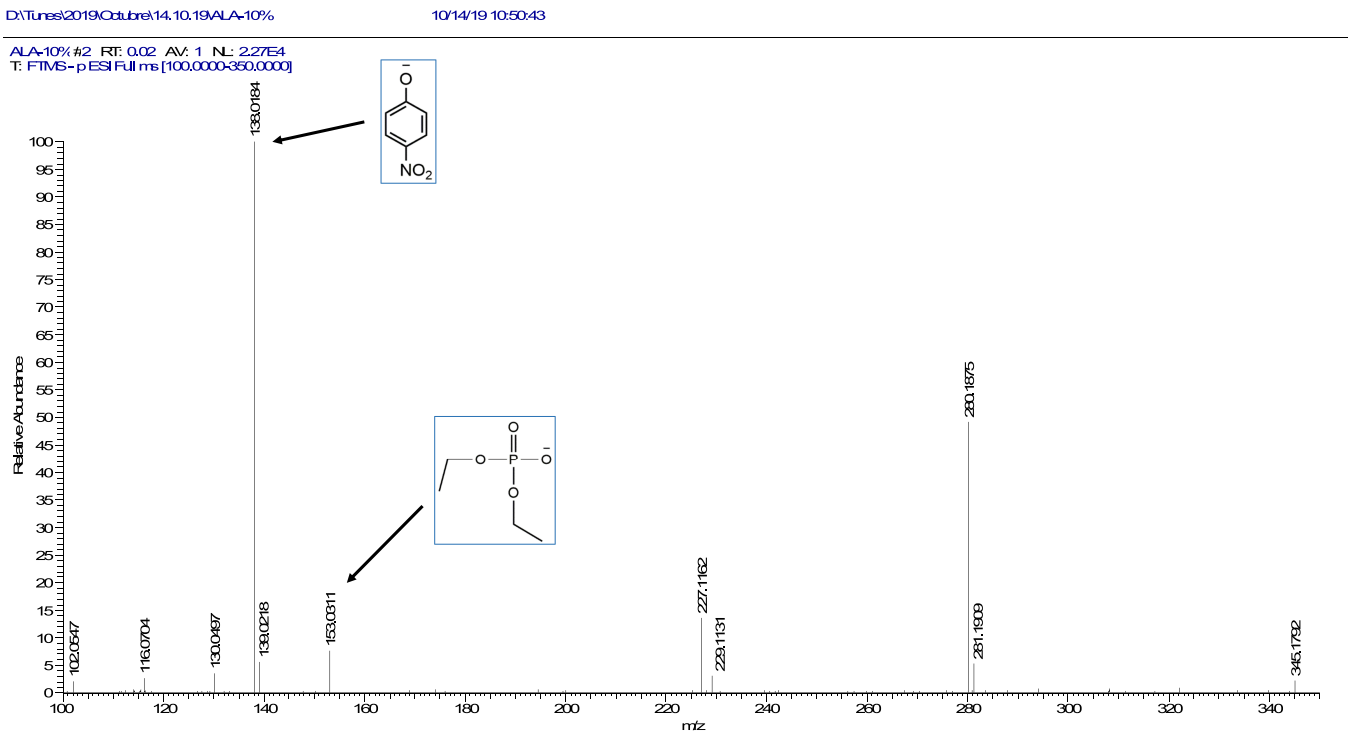

Figure 3. ESI-MS(−) spectrum of compounds **2** and 4-nitrofenolate from the reaction of Paraoxon in [Ch][Ala]/water mixtures (1 mol % IL) at 25 °C.

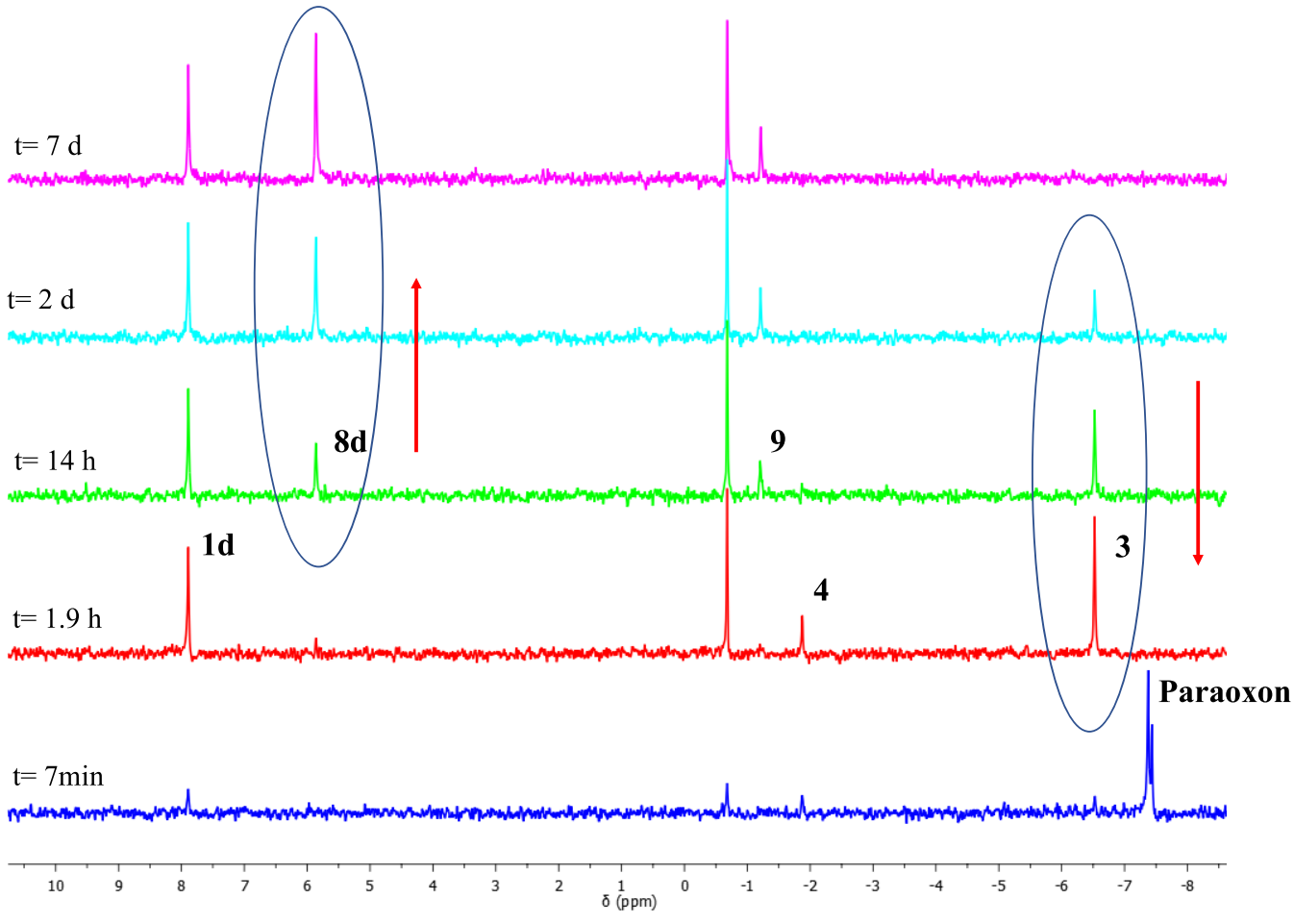

Figure 4. Stacked ^{31}P NMR plots for the reaction of Paraoxon (0.10 M) in [Ch][Pro]/water mixtures (46 mol % IL) at 25 °C.

https://dx.doi.org/10.1021/acsomega.0c03305
ACS Omega 2020, 5, 26562−26572

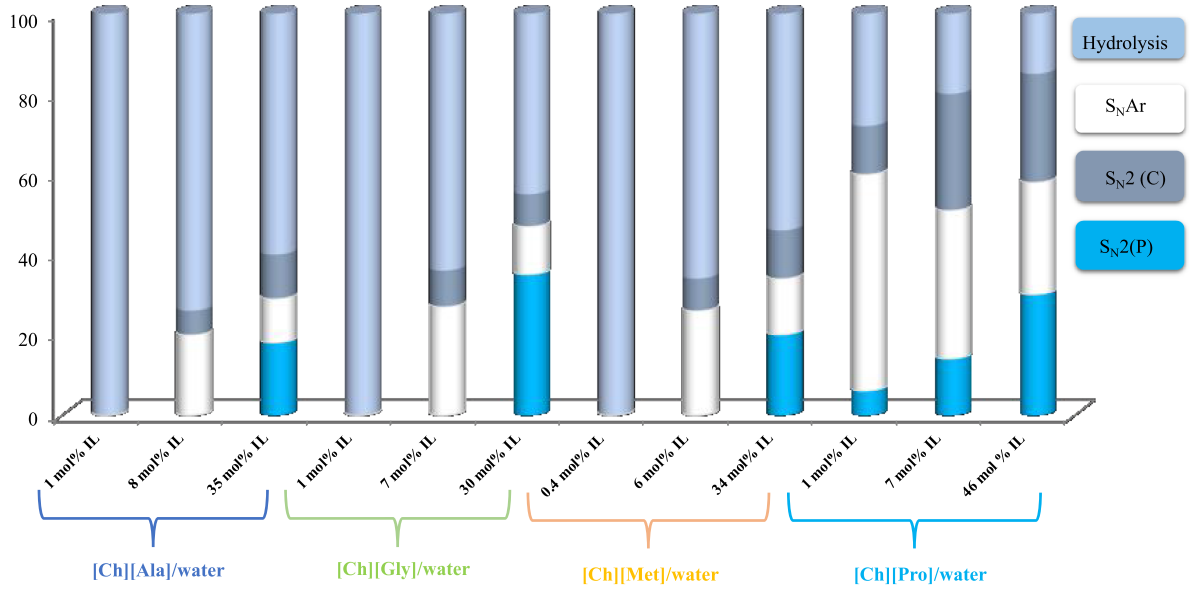

Figure 5. Relative nucleophilic attack of [Ch][AA] to Paraoxon in each [Ch][AA]/water mixture. Nucleophilic attack of [Ch][AA] at the phosphorus atom by the $S_N2(P)$ path (calypso column), at the aliphatic carbon by the $S_N2(C)$ path (gray columns), the C-1 aromatic carbon by the S_NAr path (white columns), and hydrolysis reaction (light blue columns).

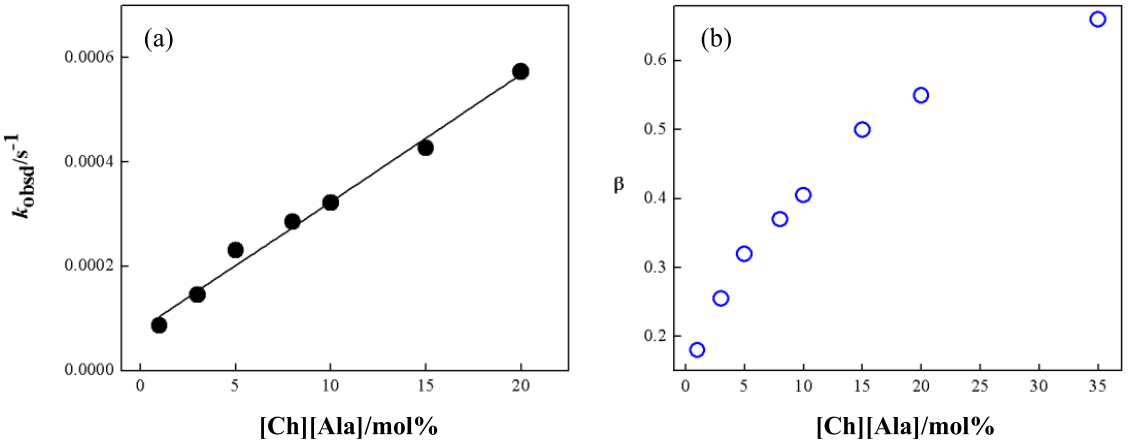

Figure 6. (a) Rate constants k_{obsd} obtained for Paraoxon degradation in [Ch][Ala]/water mixtures with varying IL contents. (b) Hydrogen bond accepting ability (β) obtained for [Ch][Ala]/water mixtures with varying IL contents. Each measurement was made in triplicate.

Table 1. Half-Life ($t_{1/2}$, min) Obtained in Paraoxon Degradation in [Ch][AA] and Those $t_{1/2}$ Values Reported in Neat Bmim[AA][21]

[Ch][AA]	$t_{1/2}$ (min) at 1 mol % IL	$t_{1/2}$ (min) at 20 mol % IL	$t_{1/2}$ (min) at 100 mol % IL	neat [Bmim][AA]	$t_{1/2}$ (min)[a]
[Ch][Gly]	175 ± 8	23 ± 1	4.5 ± 0.2	[Bmim][Gly]	[b]
[Ch][Met]	115 ± 5	27 ± 1	17.0 ± 0.8	[Bmim][Met]	[b]
[Ch][Ala]	167 ± 8	20 ± 1	4.4 ± 0.2	[Bmim][Ala]	14
[Ch][Pro]	160 ± 8	19 ± 1	4.4 ± 0.2	[Bmim][Pro]	36

[a]From ref 21. [b]Not detected by using the ^{31}P NMR technique.

acid anion (such as alanine anion in Figure 7) establishes another hydrogen bond with water, increasing the nucleophilic capacity of water. A similar catalytic effect shown in Figure 7 could be evidenced in the nucleophilic attack of water at the C-1 aromatic carbon of Paraoxon. The dual catalytic role of the

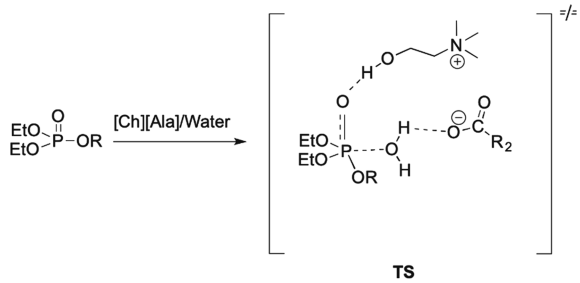

Figure 7. Hydrogen bonding interactions between cholinium cations and Paraoxon and between alaninate anions and water in the transition state (TS) of the hydrolysis step of Paraoxon.

[Ch][AA] was reported previously in a depolymerization reaction.[33]

On the other hand, as can be observed in Table 1, the kinetics result found in [Ch][Ala]/water mixtures (20 mol % IL) is close to that obtained in neat [Bmim][AA] ILs despite using aqueous mixtures of ILs. Even more, the $t_{1/2}$ value found

https://dx.doi.org/10.1021/acsomega.0c03305
ACS Omega 2020, 5, 26562−26572

for Paraoxon degradation using [Ch][Pro]/water (20 mol % IL) is 19 min, while the $t_{1/2}$ value reported in neat [Bmim][AA] ILs was 36 min.[21] Therefore, the [Ch][Pro]/water mixture (20 mol % IL) seems to be a promising alternative for faster and eco-friendly degradation of Paraoxon. The pesticide degradation occurs in an aqueous solution with a low amount of an IL made up entirely of natural sources ([Ch][AA]), without the need of an extra nucleophile, and finally, a less toxic product is formed, compound **8d**, as mentioned above.

Besides, as can be observed in Table 1, the $t_{1/2}$ values were calculated in a hypothetical [Ch][Ala] and [Ch][Pro] at 100%, showing that the Paraoxon degradation will be achieved more efficiently compared to the results reported in neat [Bmim][Ala] and neat [Bmim][Pro]. Probably, the better profile of [Ch][Ala] and [Ch][Pro] than [Bmim][Ala] and [Bmim][Pro], respectively, could be explained by the hydroxyl group present in the cholinium cation, which gives an additional possibility of hydrogen bonding interaction to stabilize a transition state and the IL acting also as a catalyst.[33]

Besides, previously, we found that the half-life values of Paraoxon degradation in several neat [Bmim][AA] decrease as the hydrogen bond accepting ability (β Kamlet−Taft parameter) of the solvent increases.[21] The β parameter describes the hydrogen bond accepting ability of the solvent. In this study, the β Kamlet−Taft descriptor to each [Ch][AA]/water mixture was determined, using a solvatochromatic dye as it has been previously reported for different ILs.[34] Figure 6b shows the effect of the [Ch][Ala] content on the β parameter. As can be observed, as the [Ch][Ala] content increases, the β value increases, in a non-linear relationship. These results suggest that content higher than 35 mol % [Ch][Ala] would not affect significantly the hydrogen bond accepting ability of these mixtures. Tables S7−S10 and Figures S22−S25 in the Supporting Information show the same behavior in [Ch][Gly]/water, [Ch][Met]/water, and [Ch][Pro]/water mixtures, respectively.

It is important to note that in this study, no correlation between the hydrogen bond accepting ability (β) of each [Ch][AA]/water mixture and the k_{obsd} values for Paraoxon degradation was found. The latter may be explained by the high water content present in the mixtures used in this study, which could be altering the hydrogen bond accepting ability of the IL. For example, the β values of those [Ch][AA]/water mixtures (20 mol % IL) (see Tables S7−S10 in the Supporting Information) are very similar to the β value reported for neat water (β = 0.5),[35] while the β values for neat [Bmim][AA] are in the range 0.8−1.1.[21]

Finally, the results show the dependence of k_{obsd} values obtained for Paraoxon degradation with the pK_a (amine group of each AA). The results show that the k_{obsd} values obtained for Paraoxon degradation in the different mixtures with a fixed [Ch][AA] content (20 mol % [Ch][AA]) follow the order [Ch][Pro]/water > [Ch][Ala]/water > [Ch][Gly]/water > [Ch][Met]/water. This sequence agrees with the scale of pK_a (in water) of the amino acids present in an IL used, pK_a (amine group) of 10.6, 9.87, 9.78, and 9.21 for [Pro], [Ala], [Gly], and [Met], respectively.[36]

CONCLUSIONS

In this study, we have demonstrated that it is possible to degrade Paraoxon in [Ch][AA]/water mixtures without the need of an extra nucleophile, even when the IL content in the mixture is low (0.4−1 mol % IL). In those mixtures with a low amount of [Ch][AA], the hydrolysis reaction is the main pathway for Paraoxon degradation. The kinetics results under these experimental conditions showed a decrease in $t_{1/2}$ values for Paraoxon hydrolysis up to three orders of magnitude in comparison with those $t_{1/2}$ values reported in aqueous solution due to a catalytic effect of the [Ch][AA] in the hydrolysis reaction of Paraoxon. Besides, as the percentage of [Ch][AA] increases in the mixture, the nucleophilic attack of [Ch][AA] is evident in the Paraoxon degradation.

Keeping in mind previous results obtained for the Paraoxon degradation using different neat [Bmim][AA] ILs, in this study, we propose a more sustainable and efficient methodology using [Ch][AA]/water mixtures (0.4−46 mol % IL) due to the following arguments: (a) the kinetics results found in [Ch][Ala]/water mixtures (20 mol % IL) are close to those obtained in neat [Bmim][Ala] ILs despite using aqueous mixtures of ILs. Even more, the $t_{1/2}$ value found for Paraoxon degradation using [Ch][Pro]/water (20 mol % IL) is 19.8 min, while the $t_{1/2}$ value reported in neat [Bmim][AA] ILs is 35.5 min; (b) the ILs used in this study ([Ch][AA]) are completely synthesized from natural resources (choline chloride and amino acids). The latter could generate a biodegradable and less toxic reaction medium than neat [Bmim][AA] ILs, and finally, (c) we have demonstrated an efficient degradation of the pesticide in a reaction medium that contains high water content and a low amount of an IL designed totally from natural resources.

EXPERIMENTAL SECTION

Reagents and Materials. All amino acids (AA) were high quality and were used as received without further purification. Choline chloride, Amberlite IRA400Cl, *O*,*O*-diethyl 4-nitrophenyl phosphate triester (Paraoxon), *O*,*O*-diethyl chlorophosphate, and standard mono- and diester phosphate derivatives were purchased. Spectroscopic grade solvatochromic dyes 4-nitroaniline (NA) and *N*,*N*-diethyl-4-nitroaniline (NN) were used as received.

Preparation and Characterization of [Ch][AA] ILs. The [Ch][AA] ILs were synthesized with some modifications according to a reported methodology.[31] The synthesis of these [Ch][AA] ILs involves two steps; the first one is an ion exchange reaction of [Ch][Cl] using Amberlite as an anion exchange resin to obtain [Ch][OH]. The second step is the neutralization of the amino acid by [Ch][OH]. [Ch][OH] was added dropwise in a slight excess of an equimolar aqueous amino acid solution to produce [Ch][AA]. The mixture was stirred at 5 °C in the dark for 48 h. Water was then removed under reduced pressure at 50 °C using a rotavapor. Then, 90 mL of acetonitrile and 10 mL of methanol were added to the solution of [Ch][AA] to separate out excess amino acid, and then, the mixture was filtered out. The filtrate was concentrated under reduced pressure at 50 °C to obtain the final product. Four [Ch][AA] ILs derived from amino acids have been synthesized in this work (see Scheme S1 in the Supporting Information). The yields of all the desired products were more than 95%.

The structures of these [Ch][AA] ILs were confirmed using ^{1}H NMR, ^{13}C NMR, and ESI-MS, see Figures S26−S37 in the Supporting Information. The water content for each [Ch][AA] (determined by Karl Fisher titration (TitroMatic)) was between 9 and 18 wt % and was considered for the preparation of all [Ch][AA]/water mixtures.

https://dx.doi.org/10.1021/acsomega.0c03305
ACS Omega 2020, 5, 26562−26572

Characterization of [Ch][AA] ILs. The NMR analysis was performed on a Bruker AVANCE-400 NMR spectrometer operating at 400 MHz for ^{1}H NMR and ^{13}C NMR. Samples were run in deuterium oxide (D_2O) where appropriate (high-resolution mass spectrometer Exactive Plus Orbitrap, Thermo-Fisher Scientific (Bremen, Germany)). The scan parameters are resolution, 140000; AGC target, 1e6; max. injection time, 200; HESI source: sheath gas flow, 30; aux. gas flow rate, 3; sweep gas flow rate, 0; capillary temp., 250 °C; S-lens RF level, 0; heater temp, 50 °C.

[Ch][Ala]. ^{1}H NMR (400 MHz, D_2O) δ: 1.25 (d, J = 7.1 Hz, 3H, CH_3), 3.22 (s, 9H, CH_3, CH_3, CH_3), 3.34 (q, J = 7.1 Hz, 1H, CH−N), 3.52−3.55 (m, 2H, CH_2), 4.06−4.10 (m, 2H, CH_2). ^{13}C NMR (400 MHz, D_2O) δ: 184.17, 67.44, 55.57, 53.92, 53.88, 53.84, 51.41, 20.38. HRMS-ESI (+ mode): found m/z, 104.1073; calculated for cation $C_5H_{14}NO$ m/z, 104.1070 (Δ = 2.9 ppm). The water content was 15 wt % and was determined using Karl Fisher titration (TitroMatic).

[Ch][Gly]. ^{1}H NMR (400 MHz, D_2O) δ: 3.17 (s, 2H, CH_2−N), 3.20 (s, 9H, CH_3, CH_3, CH_3), 3.51−3.54 (m, 2H, CH_2), 4.04−4.08 (m, 2H, CH_2). ^{13}C NMR (400 MHz, D_2O) δ: 181.00, 67.44, 55.57, 53.92, 53.88, 53.84, 44.66. HRMS-ESI (+ mode): found m/z, 104.1074; calculated for cation $C_5H_{14}NO$ m/z, 104.1070 (Δ = 3.8 ppm). The water content was 18 wt % and was determined using Karl Fisher titration (TitroMatic).

[Ch][Pro]. ^{1}H NMR (400 MHz, D_2O) δ: 1.73−1.83 (m, 3H, CH_2, CH_2), 2.11−2.19 (m, 1H, CH_2), 2.82−2.90 (m, 1H, CH_2−N), 3.07−3.15 (m, 1H, CH_2−N), 3.21 (s, 9H, CH_3, CH_3, CH_3), 3.50−3.54 (apparent t, 2H, CH_2) 3.57−3.63 (m, 1H, CH-N), 4.03−4.09 (m, 2H, CH_2). ^{13}C NMR (400 MHz, D_2O) δ: 180.75, 67.41, 61.46, 55.56, 53.89, 53.85, 53.81, 45.98, 30.40, 24.85. HRMS-ESI (+ mode): found m/z, 104.1071; calculated for cation $C_5H_{14}NO$ m/z, 104.1070 (Δ = 1.0 ppm). The water content was 9 wt % and was determined using Karl Fisher titration (TitroMatic).

[Ch][Met]. ^{1}H NMR (400 MHz, D_2O) δ: 1.78−1.88 (m, 1H, CH_2), 1.91−2.01 (m, 1H, CH_2), 2.15 (s, 3H, CH_3), 2.59 (t, J = 7.8 Hz, 2H, CH_2), 3.23 (s, 9H, CH_3, CH_3, CH_3), 3.36 (t, J = 6.4 Hz, 1H, CH−N), 3.55 (apparent t, 2H, CH_2), 4.05−4.12 (m, 2H, CH_2). ^{13}C NMR (400 MHz, D_2O) δ: 182.45, 67.45, 55.60, 55.26, 53.95, 53.91, 53.87, 34.14, 29.74, 14.14. HRMS-ESI (+ mode): found m/z, 104.1073; calculated for cation $C_5H_{14}NO$ m/z, 104.1070 (Δ = 2.9 ppm). The water content was 12 wt % and was determined using Karl Fisher titration (TitroMatic).

Determination of the β Kamlet−Taft Parameter. β Kamlet−Taft parameters of each [Ch][AA]/water mixture were determined using *N*,*N*-diethyl-4-nitroaniline (NN) and 4-nitroaniline (NA) solvatochromic dyes by the following procedure.[37]

Stock solutions of the probes were prepared in acetonitrile (5×10^{-3} mol L^{-1}). In each cell, 20 μL of the probe was added, obtaining a final concentration in the cell of 2×10^{-4} mol L^{-1}, the acetonitrile was evaporated, and then, 500 μL of each [Ch][AA]/water mixture was added. These dye-containing [Ch][AA]/water mixtures were placed in quartz cells maintained at 25 °C.

The β Kamlet−Taft parameter was obtained by measuring the relative difference of solvatochromism between 4-nitroaniline (NA) and *N*,*N*-diethyl-4-nitroaniline (NN), using eq 2.

$$\beta = \frac{(1.035\nu(\mathrm{NN})_{max} - \nu(\mathrm{NA})_{max} + 2.64)}{2.8} \quad (2)$$

Kinetics Measurements. First-order rate constants (k_{obsd}) for Paraoxon degradation in the presence of each [Ch][AA]/water mixture (approx. 1−46 mol % IL) were determined by UV−vis at 25 °C, without an extra nucleophile agent. Each measurement was made in triplicate, and the k_{obsd} values reported in Tables S2−S5 in the Supporting Information correspond to the average of the three measurements. The rate law for all the reactions studied is given by eq 3, where *P* and *S* represent one of the products and Paraoxon, respectively. In a typical experiment, 10 μL of Paraoxon (0.7 M) in acetonitrile was added to a spectroscopy cell. Acetonitrile was evaporated, and then, 700 μL of each [Ch][AA]/water mixture was added.

$$\frac{d[P]}{dt} = k_{obsd}[S] \quad (3)$$

Product Studies. *Nuclear Magnetic Resonance.* The product analysis was performed by nuclear magnetic resonance (NMR). To confirm the structural assignment of products **1a**−**d** (Scheme 2), ^{31}P NMR spectra were recorded for the reactions of *O*,*O*-diethyl chlorophosphate with each [Ch][AA] used in this study (see Figure S13 in the Supporting Information). Products **2** and **3** were confirmed by comparison of the ^{31}P NMR spectrum of the authentic sample (see Figures S14−S17 in the Supporting Information). In a typical experiment, 10 μL of Paraoxon or *O*,*O*-diethyl chlorophosphate (0.7 M) in acetonitrile was added to an NMR tube. Acetonitrile was evaporated; then, 700 μL of each [Ch][AA]/water mixture was added, and deuterated ACN was inserted via a capillary for NMR tubes.

Electrospray Ionization Mass Spectrometry (ESI-MS). The detection of **2** and compound **5** (Scheme 2), formed in the Paraoxon degradation in [Ch][Ala]/water mixtures, was undertaken on an AB Sciex Triple Quad 4500 (UHPLC−MS/MS) mass spectrometer equipped with a Turbo Ion Spray (AB Sciex) ion source. A microsyringe pump delivered the mixed reaction of Paraoxon in the presence of [Ch][Ala]/water mixtures (1 mol % IL) at an infinite time dissolved in 10% (v/v) acetonitrile into the ESI source at a flow rate of 10 μL/min.

■ ASSOCIATED CONTENT

Supporting Information

The Supporting Information is available free of charge at https://pubs.acs.org/doi/10.1021/acsomega.0c03305.

^{1}H NMR, ^{13}C NMR, ^{31}P NMR, and HRMS-ESI experiments and kinetics results (PDF)

■ AUTHOR INFORMATION

Corresponding Author

Paulina Pavez − *Facultad de Química y de Farmacia, Pontificia Universidad Católica de Chile, Santiago 6094411, Chile;* orcid.org/0000-0002-8891-3802; Phone: +56-02-23541743; Email: ppavezg@uc.cl; Fax: +56-02-26864744

Authors

Roberto Figueroa − *Facultad de Química y de Farmacia, Pontificia Universidad Católica de Chile, Santiago 6094411, Chile*

Mayte Medina − *Facultad de Química y de Farmacia, Pontificia Universidad Católica de Chile, Santiago 6094411, Chile*

https://dx.doi.org/10.1021/acsomega.0c03305
ACS Omega 2020, 5, 26562−26572

Daniela Millán − *Centro Integrativo de Biología y Química Aplicada (CIBQA), Universidad Bernardo O'Higgins, Santiago 6094411, Chile*

R. Darío Falcone − *Instituto para el Desarrollo Agroindustrial y de la Salud (IDAS), CONICET, Departamento de Química, Universidad Nacional de Río Cuarto, X5804BYA, Argentina;* orcid.org/0000-0002-0997-3437

Ricardo A. Tapia − *Facultad de Química y de Farmacia, Pontificia Universidad Católica de Chile, Santiago 6094411, Chile*

Complete contact information is available at: https://pubs.acs.org/10.1021/acsomega.0c03305

Notes

The authors declare no competing financial interest.

■ ACKNOWLEDGMENTS

This work was supported by FONDECYT grants 1170976 and 1170569 and FONDECYT postdoctoral grant 3170237, ICM-MINECON, RC-130006-CILIS Chile, Consejo Nacional de Investigaciones Científicas y Técnicas (PIP CONICET 112-2015-0100283), Universidad Nacional de Río Cuarto (PPI-UNRC 2016-2019), Agencia Nacional de Promoción Científica y Técnica (PICT 2012-0232, PICT 2012-0526, and PICT 2015-0585), Ministerio de Ciencia y Tecnología, Gobierno de la Provincia de Córdoba (PID2013 and PID2018), and the National Fund for Scientific and Technological Development.

■ REFERENCES

(1) Pacheco-Fernández, I.; Pino, V. Extraction With Ionic Liquids-Organic Compounds. In *Liquid-Phase Extraction*; Elsevier, 2020, pp. 499−537.

(2) Clarke, C. J.; Tu, W. C.; Levers, O.; Bröhl, A.; Hallett, J. P. Green and Sustainable Solvents in Chemical Processes. *Chem. Rev.* **2018**, *118*, 747−800.

(3) Hallett, J. P.; Welton, T. Room-temperature ionic liquids: solvents for synthesis and catalysis. *Chem. Rev.* **2011**, *111*, 3508−3576.

(4) Welton, T. Ionic liquids in Green Chemistry. *Green Chem.* **2011**, *13*, 225.

(5) Jordan, A.; Gathergood, N. Biodegradation of ionic liquids − a critical review. *Chem. Soc. Rev.* **2015**, *44*, 8200−8237.

(6) Egorova, K. S.; Ananikov, V. P. Toxicity of ionic liquids: Eco(cyto)activity as complicated, but unavoidable parameter for task-specific optimization. *Chem. Sus. Chem.* **2014**, *7*, 336−360.

(7) Yan, F.; Lan, T.; Yan, X.; Jia, Q.; Wang, Q. Norm index-based QSTR model to predict the eco-toxicity of ionic liquids towards Leukemia rat cell line. *Chemosphere* **2019**, *234*, 116−122.

(8) Kohno, Y.; Ohno, H. Ionic liquid/water mixtures: from hostility to conciliation. *Chem. Commun.* **2012**, *48*, 7119−7130.

(9) Reddy, P. N.; Padmaja, P.; Subba Reddy, B. V.; Rambabu, G. Ionic liquid/water mixture promoted organic transformations. *RSC Adv.* **2015**, *5*, 51035−51054.

(10) Keaveney, S. T.; Greaves, T. L.; Kennedy, D. F.; Harper, J. B. Understanding the Effect of Solvent Structure on Organic Reaction Outcomes When Using Ionic Liquid/Acetonitrile Mixtures. *J. Phys. Chem. B* **2016**, *120*, 12687−12699.

(11) Keaveney, S. T.; Haines, R. S.; Harper, J. B. Ionic liquid solvents: the importance of microscopic interactions in predicting organic reaction outcomes. *Pure Appl. Chem.* **2017**, *89*, 745−757.

(12) Schaffarczyk McHale, K. S.; Haines, R. S.; Harper, J. B. The dependence of ionic liquid solvent effects on the nucleophilic heteroatom in SNAr reactions. Highlighting the potential for control of selectivity. *ChemPlusChem* **2019**, *84*, 465−473.

(13) Gilbert, A.; Haines, R. S.; Harper, J. B. Understanding the effects of ionic liquids on a unimolecular substitution process: correlating solvent parameters with reaction outcome. *Org. Biomol. Chem.* **2019**, *17*, 675−682.

(14) Gilbert, A.; Haines, R. S.; Harper, J. B. Controlling the reactions of 1-bromogalactose acetate in methanol using ionic liquids as cosolvents. *Org. Biomol. Chem.* **2020**, *18*, 5442−5452.

(15) Harifi-Mood, A. R.; Habibi-Yangjeh, A.; Gholami, M. R. Kinetics study of a Diels-Alder reaction in mixtures of an ionic liquid with molecular solvents. *J. Phys. Org. Chem.* **2008**, *21*, 783−788.

(16) Ohno, H.; Fukumoto, K. Amino acid ionic liquids. *Acc. Chem. Res.* **2007**, *40*, 1122−1129.

(17) Fukumoto, K.; Yoshizawa, M.; Ohno, H. Room temperature ionic liquids from 20 natural amino acids. *J. Am. Chem. Soc.* **2005**, *127*, 2398−2399.

(18) Fukaya, Y.; Iizuka, Y.; Sekikawa, K.; Ohno, H. Bio ionic liquids: room temperature ionic liquids composed wholly of biomaterials. *Green Chem.* **2007**, *9*, 1155−1157.

(19) Poletti, L.; Chiappe, C.; Lay, L.; Pieraccini, D.; Polito, L.; Russo, G. Glucose-derived ionic liquids: exploring low-cost sources for novel chiral solvents. *Green Chem.* **2007**, *9*, 337−341.

(20) Hulsbosch, J.; De Vos, D. E.; Binnemans, K.; Ameloot, R. Biobased ionic liquids: Solvents for a green processing industry? *ACS Sustainable Chem. Eng.* **2016**, *4*, 2917−2931.

(21) Morales, J. I.; Figueroa, R.; Rojas, M.; Millán, D.; Tapia, R. A.; Pavez, P. Dual function of amino acid ionic liquids (Bmim[AA]) on the degradation of the organophosphorus pesticide, Paraoxon®. *Org. Biomol. Chem.* **2018**, *16*, 7446−7453.

(22) Liu, Q.-P.; Hou, X.-D.; Li, N.; Zong, M.-H. Ionic liquids from renewable biomaterials: synthesis, characterization and application in the pretreatment of biomass. *Green Chem.* **2012**, *14*, 304−307.

(23) Gontrani, L. Choline-amino acid ionic liquids: past and recent achievements about the structure and properties of these really "green" chemicals. *Biophys. Rev.* **2018**, *10*, 873−880.

(24) Jordan, A.; Haiß, A.; Spulak, M.; Karpichev, Y.; Kümmerer, K.; Gathergood, N. Synthesis of a series of amino acid derived ionic liquids and tertiary amines: green chemistry metrics including microbial toxicity and preliminary biodegradation data analysis. *Green Chem.* **2016**, *18*, 4374−4392.

(25) Tanner, E. E. L.; Piston, K. M.; Ma, H.; Ibsen, K. N.; Nangia, S.; Mitragotri, S. The Influence of Water on Choline-Based Ionic Liquids, ACS Biomater. *ACS Biomater. Sci. Eng.* **2019**, *5*, 3645−3653.

(26) Pavez, P.; Millán, D.; Morales, J. I.; Castro, E. A.; López, C.; Santos, J. G. Mechanisms of degradation of paraoxon in different ionic liquids. *J. Org. Chem.* **2013**, *78*, 9670−9676.

(27) Brotzel, F.; Chu, Y. C.; Mayr, H. Nucleophilicities of primary and secondary amines in water. *J. Org. Chem.* **2007**, *72*, 3679−3688.

(28) Brotzel, F.; Mayr, H. Nucleophilicities of amino acids and peptides. *Org. Biomol. Chem.* **2007**, *5*, 3814−3820.

(29) Gupta, A.; Kaur, S.; Kashyap, H. K. How Water Permutes the Structural Organization and Microscopic Dynamics of Cholinium Glycinate Biocompatible Ionic Liquid. *J. Phys. Chem. B* **2019**, *123*, 2057−2069.

(30) Lyznicki, E. P., Jr.; Oyama, K.; Tidwell, T. T. Reactivity of Organophosphates. IV. Acid-catalyzed Hydrolysis of Triethyl Phosphate: a Comparison with Ethyl Acetate. *Can. J. Chem.* **1974**, *52*, 1066.

(31) De Santis, S.; Masci, G.; Casciotta, F.; Caminiti, R.; Scarpellini, E.; Campetella, M.; Gontrani, L. Cholinium-amino acid based ionic liquids: A new method of synthesis and physico-chemical characterization. *Phys. Chem. Chem. Phys.* **2015**, *17*, 20687−20698.

(32) Druzina, B.; Stegu, M. Degradation study of selected organophosphorus insecticides in natural waters. *Int. J. Environ. Anal. Chem.* **2007**, *87*, 1079−1093.

(33) Ferreira, R.; Garcia, H.; Sousa, A. F.; Guerreiro, M.; Duarte, F. J. S.; Freire, C. S. R.; Calhorda, M. J.; Silvestre, A. J. D.; Kunz, W.; Rebelo, L. P. N.; Silva Pereira, C. Unveiling the dual role of the cholinium hexanoate ionic liquid as solvent and catalyst in suberin depolymerisation. *RSC Adv.* **2014**, *4*, 2993−3002.

(34) Rani, M. A. A.; Brant, A.; Crowhurst, L.; Dolan, A.; Lui, M.; Hassan, N. H.; Hallett, J. P.; Hunt, P. A.; Niedermeyer, H.; Perez-Arlandis, J. M.; Schrems, M.; Welton, T.; Wilding, R. Understanding the polarity of ionic liquids. *Phys. Chem. Chem. Phys.* **2011**, *13*, 16831−16840.
(35) Buhvestov, U.; Rived, F.; Ràfols, C.; Bosch, E.; Rosés, M. Solute-Solvent and Solvent-Solvent Interactions in Binary Solvent Mixtures. *J. Phys. Org. Chem.* **1998**, *11*, 185−192.
(36) Lide, D. R. *CRC handbook of chemistry and physics: a ready-reference book of chemical and physical data;* CRC Press, 2004, vol. *41*.
(37) Rai, R.; Pandey, S. Solvatochromic probe response within ionic liquids and their equimolar mixtures with tetraethylene glycol. *J. Phys. Chem. B* **2014**, *118*, 11259−11270.

https://dx.doi.org/10.1021/acsomega.0c03305
ACS Omega 2020, 5, 26562−26572